Journal of Solid State Chemistry 183 (2010) 57–64

Contents lists available at ScienceDirect

Journal of Solid State Chemistry

journal homepage: www.elsevier.com/locate/jssc

TiO_2 nanotube, nanowire, and rhomboid-shaped particle thin films fixed on a titanium metal plate

Yuko Inoue [a], Iwao Noda [b], Toshio Torikai [a], Takanori Watari [a], Takao Hotokebuchi [c], Mitsunori Yada [a,*]

[a] Saga University, Department of Chemistry and Applied Chemistry, Faculty of Science and Engineering, 1 Honjo, Saga 840-8502, Japan
[b] Japan Medical Materials Corporation, Uemura Nissei Bldg. 9F 3-3-31 Miyahara, Yodogawa-ku, Osaka 532-0003, Japan
[c] Saga University, Department of Orthopaedic Surgery, Faculty of Medicine, 5 Nabeshima, Saga 849-8501, Japan

ARTICLE INFO

Article history:
Received 7 August 2009
Received in revised form
10 October 2009
Accepted 25 October 2009
Available online 31 October 2009

Keywords:
Titanium dioxide
Nanotube
Nanowire
Thin film

ABSTRACT

Titanium dioxide thin films having various nanostructures could be formed by various treatments on sodium titanate nanotube thin films approximately 5 μm thick fixed on titanium metal plates. Using an aqueous solution with a lower hydrochloric acid concentration (0.01 mol/L) and a higher reaction temperature (90 °C) than those previously employed, we obtained a hydrogen titanate nanotube thin film fixed onto a titanium metal plate by H^+ ion-exchange treatment of the sodium titanate nanotube thin film. Calcination of hydrogen titanate nanotube thin films yielded porous thin films consisting of anatase nanotubes, anatase nanowires, and anatase nanoparticles grown directly from the titanium metal plate. H^+ ion-exchange treatment of sodium titanate nanotube thin films at 140 °C resulted in porous thin films consisting of rhomboid-shaped anatase nanoparticles.

1. Introduction

Titanium compounds with one-dimensional nanostructures, such as nanotubes and nanofibers, have recently attracted significant interest. Among these compounds, nanotubes composed of titanium dioxide and titanate are now being studied actively. Titanium dioxide nanotubes can be synthesized using porous anodic alumina membranes [1,2], organic molecules [3], or polycarbonate membranes [4] as templates, or methods involving anodization of titanium metals [5,6]. Since the interesting reports by Kasuga et al. [7,8] and Chen et al. [9], titanate and titanium dioxide nanotubes synthesized using the hydrothermal method have found a wide range of potential uses in photocatalysis [10,11], dye sensitizing solar batteries [12], hydrogen storage [13], electrochromism [14], bonelike apatite formation [15], proton conductors [16], electron field emission characteristic [17], photoinduced hydrophilicity [18], etc.

To maximize and make effective use of the characteristics of titanate and titanium dioxide nanotubes synthesized by the hydrothermal method, it is important to fabricate thin films composed of nanotubes. Kasuga et al. [19] reported the fabrication of titanate nanotube thin films by coating a titanate nanotube dispersion liquid to a substrate, and then calcinating the substrate. Tokudome et al. [14] and Ma et al. [20] also reported the fabrication of titanate nanotube thin films using a layer-by-layer method. However, neither study had transformed titanate nanotube thin films into titanium dioxide thin films. Kim et al. [21] used electrophoretic deposition (EPD) to fabricate 2-μm-thick titanate nanotube thin films, and they transformed the titanate nanotube thin films into titanium dioxide nanotube thin films by calcination. However, these methods involve complicated processes, including (1) synthesis of nanotubes, (2) preparation of a liquid in which the synthesized nanotubes are dispersed, (3) coating of the nanotubes onto a substrate using the prepared liquid, and (4) fixation of the coated nanotubes onto the substrate surface by calcination. Since it is generally difficult to prepare a liquid in which nanotubes are uniformly dispersed and that partial aggregation is inevitable, the homogeneity of thin films thus formed is questionable. Moreover, permanent fixation of the thin films onto the substrates is also doubtful.

Titanate and titanium dioxide nanotube thin films can also be formed on titanium metal by immersing titanium metal as a raw material into NaOH aqueous solution and then performing hydrothermal treatment [17,22–25]. The fabrication of titanate nanotube thin films using titanium metal plates was first reported by Tian et al. [22]. The thin (~10 μm) films were detached from the titanium metal plates by hydrothermal reaction in 10 mol/L NaOH solution at 150 °C for 20 h. In contrast, thin films obtained by a short (6 h) hydrothermal reaction in 10 mol/L NaOH solution at 150 °C strongly adhered to the titanium metal plate. Miyauchi et al. [17] obtained a titanium dioxide nanotube thin film by hydrothermal treatment on titanium metal in NaOH solution,

* Corresponding author.
E-mail address: yada@cc.saga-u.ac.jp (M. Yada).

0022-4596/$ - see front matter © 2009 Elsevier Inc. All rights reserved.
doi:10.1016/j.jssc.2009.10.028

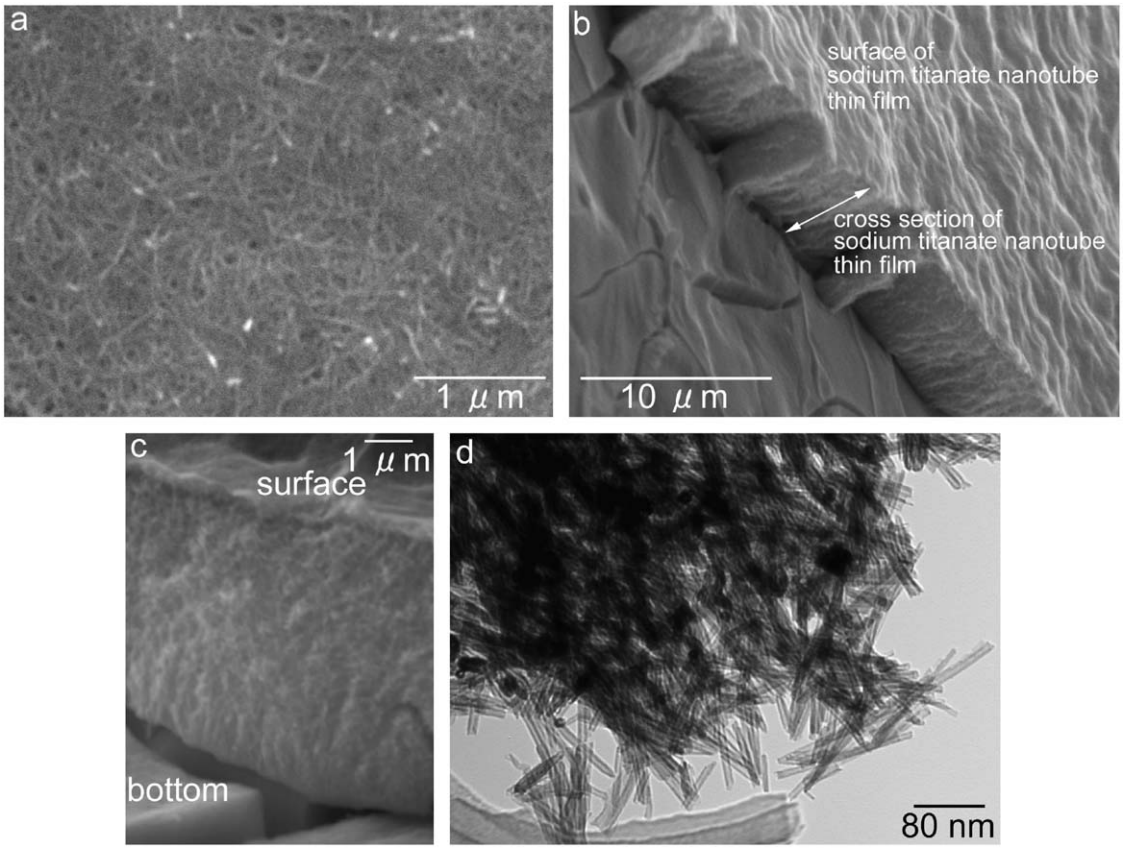

Fig. 1. SEM (a–c) and TEM (d) images of the as-grown thin film. (a) surface, (b, c) cross-section.

followed by acid treatment and calcination. The obtained thin film consisted of oriented titanium dioxide nanotubes oriented almost perpendicular to the titanium metal surface. Although this thin film was fixed onto the substrate, its thickness was only a few hundred nanometers. Chi et al. [23] also reported the fabrication of a sodium titanate nanotube thin film on a titanium metal plate by hydrothermal treatment of a titanium metal plate in NaOH solution. However, the thickness of the obtained film was not mentioned in their report, and the sodium titanate nanotubes were not transformed into titanium dioxide nanotubes. In our previous study [24], we succeeded in forming a sodium titanate nanotube thin film approximately 20 μm thick and fixed it onto a titanium metal plate using the following method: (1) after hydrothermal treatment on a titanium metal plate in 10 mol/L NaOH solution at 160 °C for 20 h, the resulting sample is dried, without washing with water; (2) the dried sample is calcined at 300 °C; and (3) the sample is washed with water to remove excess NaOH adhering to the thin film. We have also demonstrated that the thickness of the sodium titanate nanotube thin film can be adjusted by changing the duration of the hydrothermal reaction [24]. The obtained films were thicker than those reported in previous studies [17,22]. The thin film detached from the substrate when washed with water immediately after the hydrothermal reaction, similar to the result reported by Tian et al. [22]. Although thin films obtained by hydrothermal reaction in 10 mol/L NaOH solution at 160 °C for 1 h do not detach from the substrates even when washed with large amounts of water, they remain as thin as approximately 1 μm. Therefore, it is clear that sodium titanate nanotube thin films tend to detach from the substrates when they become too thick, but remain firmly fixed on substrates when the obtained samples are dried (without washing with water) and subsequently calcined at 300 °C. The next step is to transform the titanate nanotube thin films into titanium dioxide nanotube thin films. After our report [24], Guo et al. [25] reported an 8-μm-thick sodium titanate nanotube thin film on a titanium flake, but they did not transform it into a titanium dioxide nanotube thin film. To date, no report exists on the transformation of titanate nanotube thin films into titanium dioxide thin films [22–25].

We report herein the formation of titanium dioxide thin films composed of various nanostructures fabricated by treating sodium titanate nanotube thin films fixed onto titanium metal plates. In particular, we introduce a new method for transforming approximately 5-μm-thick sodium titanate nanotube thin films [24,26] into titanium dioxide nanotube thin films. We demonstrate that to obtain an anatase nanotube thin film, it is necessary to slightly modify previously reported methods for synthesizing titanium dioxide nanotube particles. Synthetic methods used to generate thin films consisting of anatase nanowires, anatase nanoparticles, and rhomboid-shaped anatase nanoparticles are also introduced.

2. Experimental procedure

One of our aims in the current study is to synthesize titanium dioxide nanotube thin films with a thickness of at least a few micrometers or more, which is thicker than those reported in previous studies [17,21]. Therefore, by hydrothermal reaction in 10 mol/L NaOH solution at 160 °C for 3 h, we prepared the previously reported [24,26] approximately 5-μm-thick sodium titanate nanotube thin film fixed on a titanium metal plate. We then transformed the fixed sodium titanate nanotube thin film into a titanium dioxide nanotube thin film.

A titanium metal plate (2 cm × 2 cm × 2 mm, Japan Medical Materials Corp.) was immersed in 20 ml of 10 mol/L NaOH

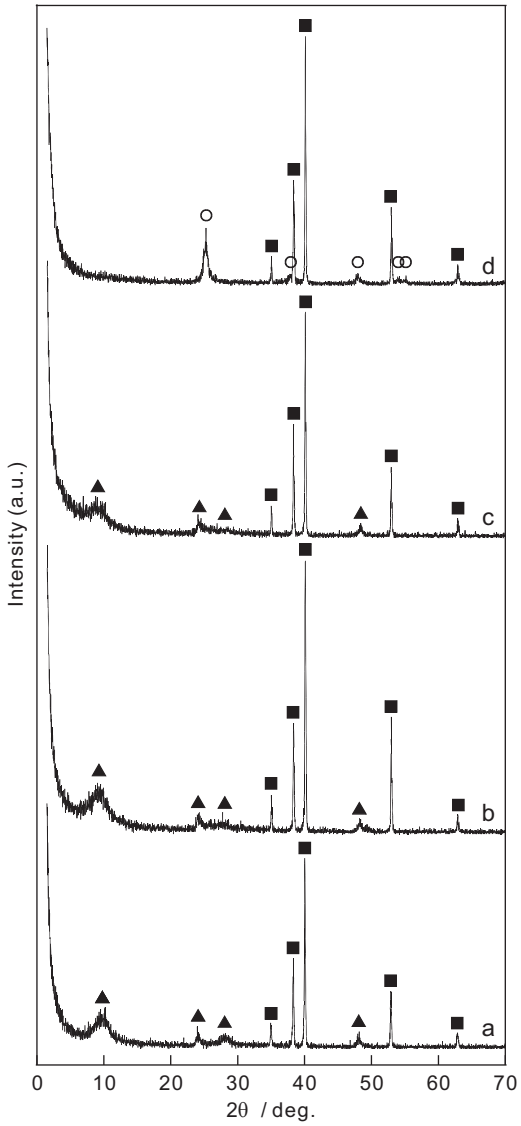

Fig. 2. XRD patterns of the as-grown (a) and the ion-exchange-treated thin films at 40 °C (b), 90 °C (c), and 140 °C (d). Peak assignment: ■, α-titanium; ○, anatase; ▲, titanate.

aqueous solution, and hydrothermal reaction was carried out at 160 °C for 3 h. After taking the sample out of a container for the hydrothermal reaction, the sample was soaked in a container with approximately 5 ml of water for a few seconds. Immediately after soaking, the water was discarded. This process was repeated twice, and the sample was then dried in air. The temperature was then increased to 300 °C at a heating rate of 1 °C/min, and the sample was calcined at 300 °C for 3 h and then washed with water to remove excess NaOH on the plates. The resulting sample consisted of a sodium titanate nanotube thin film on the plate, which was then immersed in 20 ml of 0.01 mol/L hydrochloric acid solution at 40, 90, and 140 °C for 3 h to allow an ion-exchange reaction between Na^+ ions in sodium titanate and H^+ ions in the hydrochloric acid solution. For the ion-exchange reaction at 40 °C, 0.1 and 1.0 mol/L hydrochloric acid solutions were also used. After the reaction was complete, the samples were repeatedly washed with water to remove excess ions, and were at this point termed "ion-exchange-treated" samples. The samples were calcined at 300, 450, 600, 750, or 900 °C for 1 h to transform the hydrogen titanate into titanium dioxide.

Transmission electron microscopy (TEM) was performed on a JEOL JEM-1210 instrument, scanning electron microscopy (SEM) on a Hitachi S-3000N instrument, energy-dispersive X-ray microanalysis (EDX) on an EDAX Genesis 2000 instrument, and powder X-ray diffraction (XRD) on a Shimadzu XRD-6100 instrument with Cu$K\alpha$ radiation.

3. Results and discussion

3.1. Synthesis of sodium titanate nanotube thin films

A thin film was formed uniformly over the entire sample surface, as shown in Supporting Information (Fig. S1a). The SEM image (Fig. 1a–c) confirms the formation of a uniform porous thin film approximately 5 μm thick, consisting of fibrous particles on the sample surface. Although a dense phase is observed at the bottom of the thin film (i.e., at the interface between the nanotube phase and the titanium metal) as shown in Fig. 1c, the porous structure composed of fibrous particles is observed in the film itself. The TEM image (Fig. 1d) shows that the fibrous particles are nanotubes with an average outer diameter of 8.3 nm and an average inner diameter of 3.3 nm. The XRD pattern (Fig. 2a) shows four diffraction peaks (2θ=9.6°, 24.1°, 28.5°, and 48.1°) attributed to titanate [9,27], together with peaks attributed to α-titanium (JCPDS No. 44–1294). EDX analysis indicates a molar ratio Na:Ti:O=1.0:2.1:4.8, suggesting that the product consists of sodium titanate nanotubes with the chemical composition $Na_2Ti_4O_9 \cdot H_2O$ [27]. These results are almost identical to our previously reported results [24,26]. Detailed formation mechanism of the sodium titanate nanotube thin film and the nanostructures of the thin film on the inside and at the bottom of the nanotubes and at the boundary between the titanium metal plate and the titanate nanotube thin film have already been described in our previous reports [24].

3.2. H^+ ion-exchange treatment for sodium titanate nanotube thin films

To transform sodium titanate nanotubes into hydrogen titanate nanotubes by acid treatment, it is common to use H^+ ion-exchange treatment with a 0.1 mol/L hydrochloric acid or nitric acid solution. [7,8,10,12,14,16–19]. Since temperature for the H^+ ion-exchange treatment has not been stated [7,8,10,12,14,16–19], it is presumed that the the H^+ ion-exchange treatment was performed at room temperature. In our experiment, fabricating samples by H^+ ion-exchange treatment at 40 °C for 3 h using 0.01 and 0.1 mol/L hydrochloric acid solutions resulted in nanotube films, as shown in Fig. 3a and b, respectively. However, the ratios of sodium to titanium were Na/Ti=0.14 for the 0.01 mol/L hydrochloric acid solution and Na/Ti=0.05 for the 0.1 mol/L hydrochloric acid solution, respectively. This means that substantial amounts of Na^+ ions remained in the samples after treatment. We therefore performed the H^+ ion-exchange treatment with a higher hydrochloric acid concentration to complete the H^+ ion-exchange reaction. However, after treatment using 1.0 mol/L hydrochloric acid solution, the nanotube thin films detached from the titanium metal plate, as shown in Fig. 3c. A dense titanium oxyhydroxide phase or a dense sodium titanate phase that does not consist of nanotubes is known to exist at the boundary between sodium titanate nanotubes grown from the titanium metal and the titanium metal itself [17,24,25]. It has also been reported that when titanates are treated with strong acid, their crystal structure changes to anatase [28]. The ion-exchange treatment with highly concentrated (1.0 mol/L) hydrochloric acid

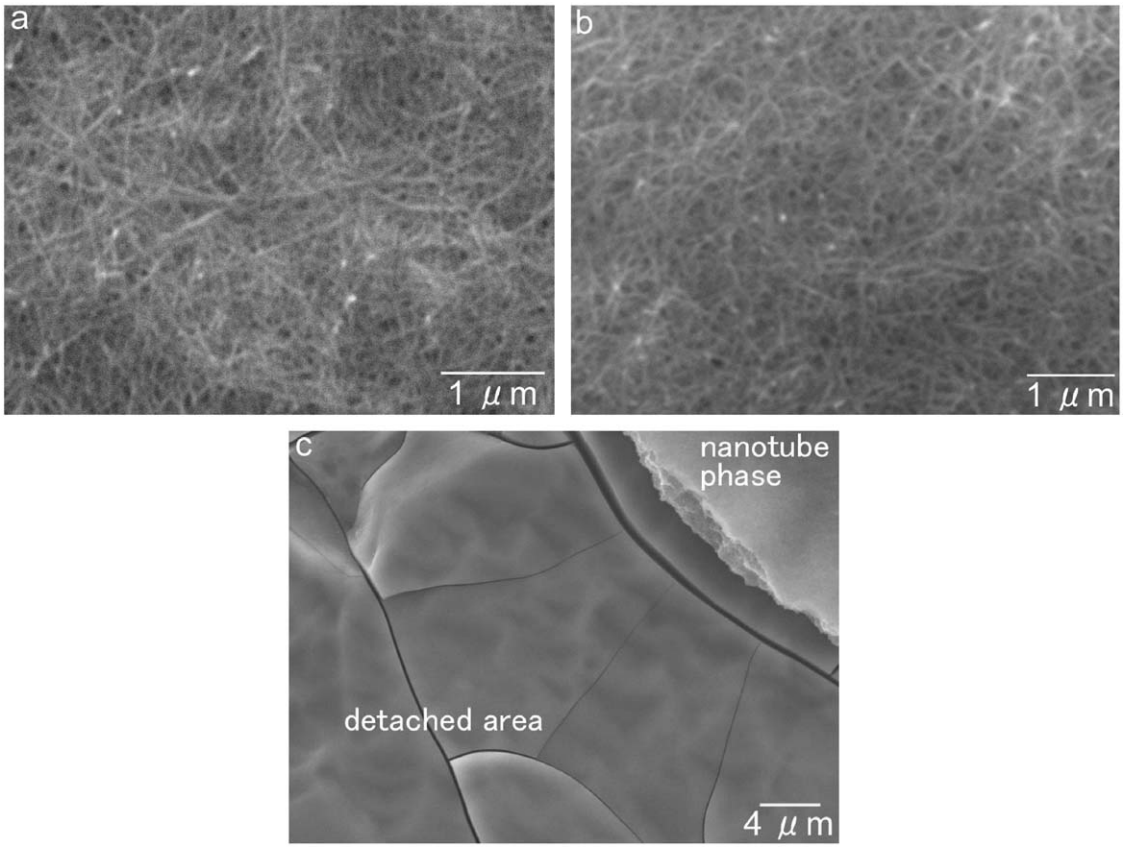

Fig. 3. SEM images of the ion-exchange-treated thin films at 40 °C at 0.01 mol/L (a), 0.1 mol/L (b), and 1 mol/L (c) hydrochloric acid solution.

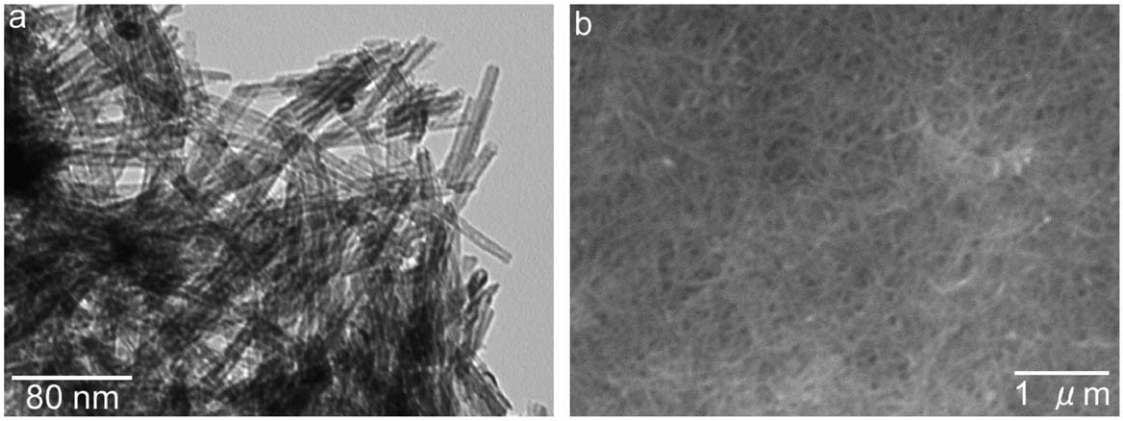

Fig. 4. TEM (a) and SEM (b) images of the ion-exchange-treated thin film at 90 °C.

solution causes a rapid change in the crystal structure, accompanied by a polycondensation reaction in the phase at the boundary, causing the boundary to rapidly contract, and consequently, the thin film detaches from the titanium metal plate. We therefore conclude that the H^+ ion-exchange treatments at 40 °C were unsuccessful.

To prevent this rapid contraction of the phase at the boundary, it would be preferable to perform the H^+ ion-exchange treatment with a low concentration hydrochloric acid solution (0.01 mol/L). In a general ion-exchange reaction at a high temperature, the kinetic energy of ions is large so the reaction proceeds faster. Therefore, we presumed that elevated temperature assists the diffusion of ions, allowing ion-exchange to occur within the deepest regions of the film, and performed H^+ ion-exchange treatment using 0.01 mol/L hydrochloric acid solution at 90 and 140 °C for 3 h. The thin films resulting from treatment at these two temperatures remain attached over the entire surface of each sample, as shown in Supporting Information (Fig. S1b and c). EDX analysis reveal that because the molar ratio of Na/Ti decrease from 0.48 before treatment to 0 after treatment at 90 and 140 °C, Na^+ ions between titanate layers are confirmed to be completely exchanged for H^+ ions. The temperature required for the complete H^+ ion-exchange reaction would be higher than that previously reported [7,8,10,12,14,16–19].

We observe nanotubes with an average outer diameter of 8.3 nm and inner diameter of 3.3 nm in the ion-exchange-treated sample at 90 °C (Fig. 4a), similar to what is observed before ion-exchange treatment (Fig. 1d). No change is observed in the porous

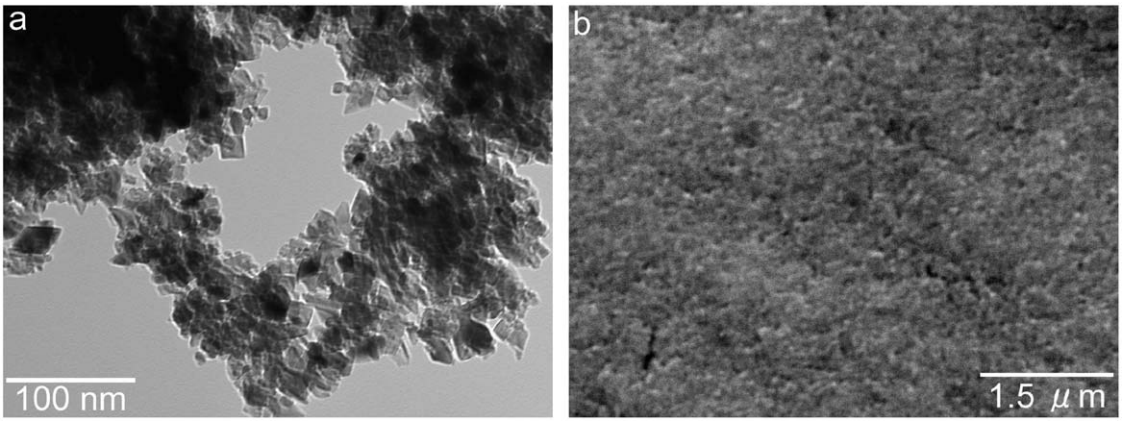

Fig. 5. TEM (a) and SEM (b) images of the ion-exchange-treated thin film at 140 °C.

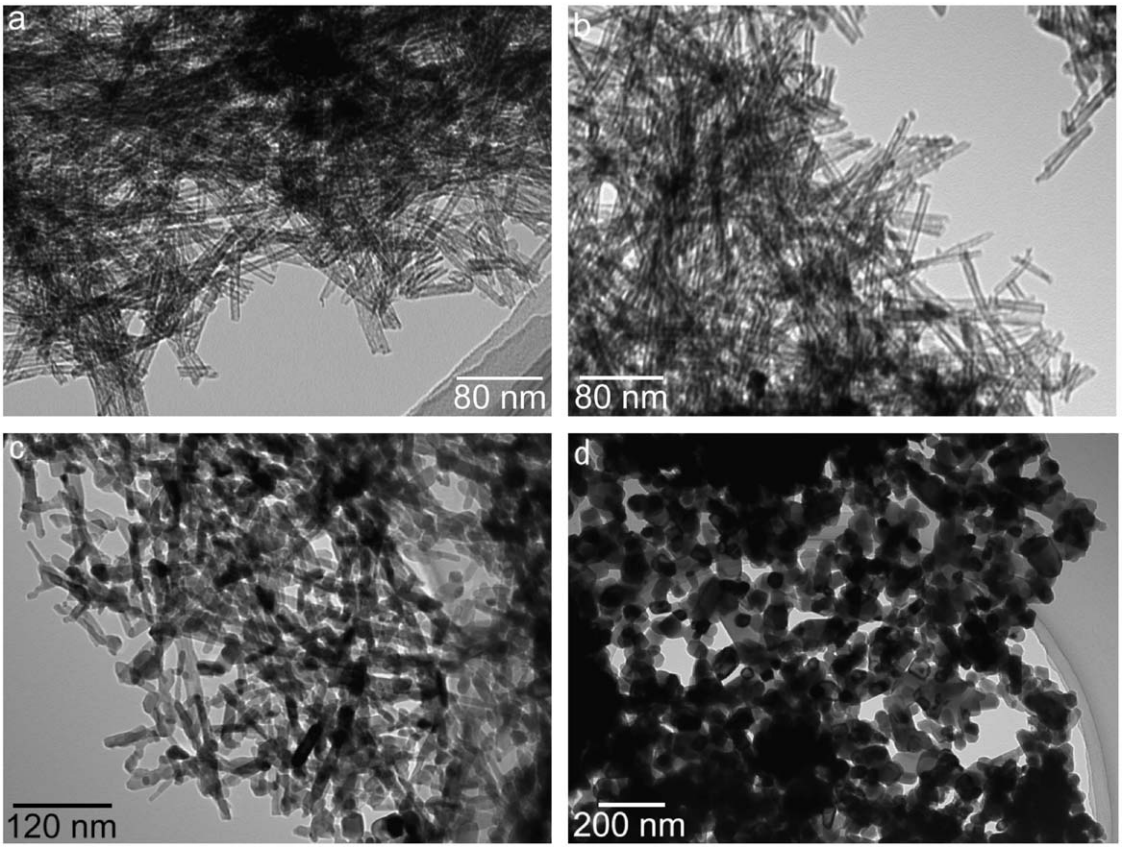

Fig. 6. TEM images of the 90 °C ion-exchange-treated thin films calcined at 300 °C (a), 450 °C (b), 600 °C (c), and 750 °C (d).

structure of the thin film before or after treatment (Figs. 1a and 4b). The porous structure consists of pores in the gaps between fibrous particles. The XRD pattern (Fig. 2c) for the H^+ ion-exchanged sample at 90 °C shows four diffraction peaks (near 2θ=9°, 24°, 29°, and 48°) attributed to titanate together with peaks attributed to α-titanium, similar to those for the as-grown sample (Fig. 2a) and the H^+ ion-exchanged sample at 40 °C (Fig. 2b). We therefore believe that the H^+ ion-exchange treatment at 90 °C transforms sodium titanate nanotubes into hydrogen titanate nanotubes while maintaining the crystal structure of titanate, nanotubular morphology, and porous thin-film structure.

In contrast, the H^+ ion-exchange treatment at 140 °C replaces the fibrous morphology with rhomboid-shaped particles (average diameter 21 nm) (Fig. 5a) and pores (~45 nm diameter) in the interstitial gaps (Fig. 5b). The XRD pattern of this sample (Fig. 2d) shows no diffraction peaks attributed to titanate, but shows peaks attributed to anatase (JCPDS no. 21–1272). Therefore, a porous thin film consisting of rhomboid-shaped anatase is confirmed to be formed on the titanium metal plate. Change in the crystal structure of sodium titanate nanotubes to anatase particles by acid treatment have been described previously by Tsai et al. [28]. They reported that although a titanate nanotube form is maintained by acid treatment at pH 1.6, only irregular-shaped anatase particles are formed by acid treatment at pH 0.38. Zhu et al. [29] reported that hydrogen titanate nanofiber transforms into anatase nanocrystals in dilute (0.05 mol/L) HNO_3 at 80–120 °C. They stated that monodispersed anatase nanocrystals are obtained at 80 °C and

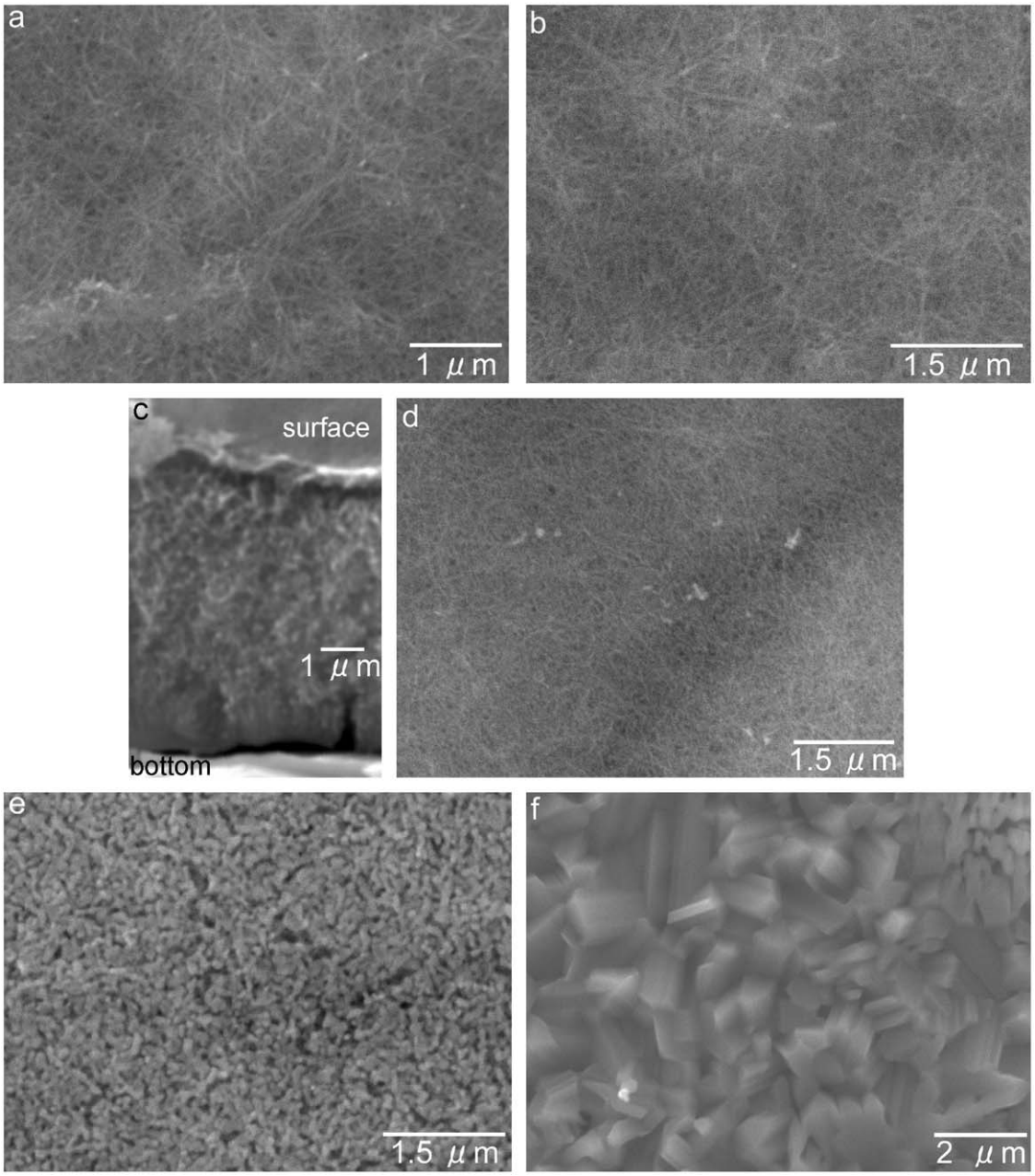

Fig. 7. SEM images of the 90 °C ion-exchange-treated thin films calcined at 300 °C (a), 450 °C (b, c), 600 °C (d), 750 °C (e), and 900 °C (f).

aggregates of nanocrystals are obtained at 120 °C. Our results also suggest that the change in the crystal structure change of titanate compounds to anatase is determined not only by pH but also by the temperature of the ion-exchange treatment. We suggest that the high temperature (140 °C) of the ion-exchange treatment is responsible for the change in the crystal structure of hydrogen titanate to the anatase structure, with a high degree of crystallization, and that this change occurs due to polycondensation and dissolution–redeposition reactions. Thus, we conclude that the complete H^+ ion-exchange is successful at elevated temperatures.

3.3. Calcination of hydrogen titanate nanotube thin films

Next, the hydrogen titanate nanotube thin films obtained by H^+ ion-exchange treatment at 90 °C using a 0.01 mol/L solution of hydrochloric acid were calcined at 300–900 °C for 3 h in air to transform them into titanium dioxide nanotube thin films. A uniform thin film formed on each sample surface, similar to the sample before calcination. Digital camera images of the calcined thin films are shown in Supporting Information (Fig. S1d–h). TEM images show that calcination at 300 and 450 °C (Fig. 6a and b) yields nanotubes. Although the average inner diameter of 3.3 nm for nanotubes synthesized by calcination at 450 °C is similar to that of the as-grown sodium titanate nanotubes, the average outer diameter of the nanotubes decreased from 8.3 nm for the as-grown thin film to 8.1 nm for the nanotubes synthesized by calcination at 450 °C. This slight decrease in the average outer diameter may be due to a phase transition from titanate into titanium dioxide. Calcination at 600 °C (Fig. 6c) yields nanofibers approximately 11 nm thick, but not nanotubes. Calcination at 750 °C (Fig. 6d) yields aggregates wherein particles with an average length of 47 nm replace the one-dimensional

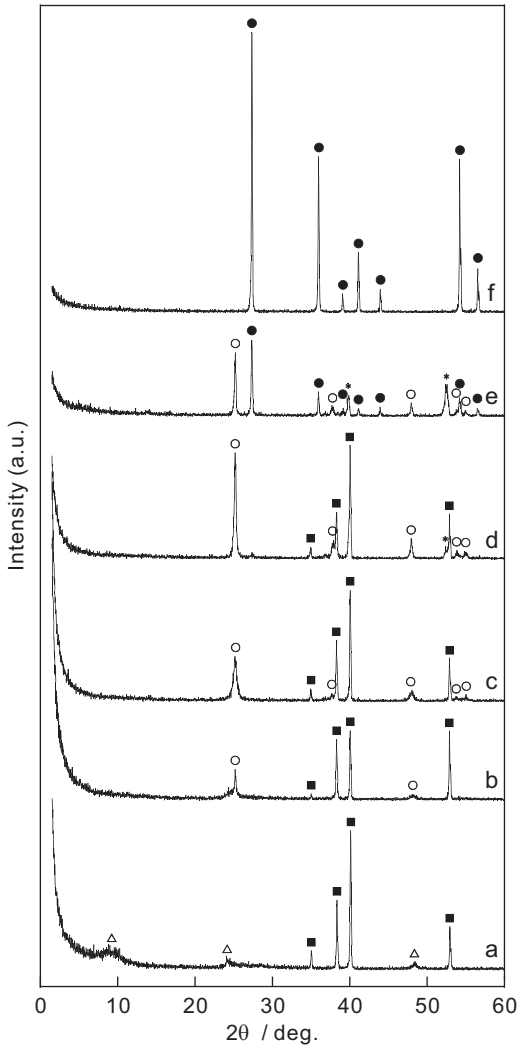

Fig. 8. XRD patterns of the 90 °C ion-exchange-treated (a) and the 90 °C ion-exchange-treated thin films calcined at 300 °C (b), 450 °C (c), 600 °C (d), 750 °C (e), and 900 °C (f). Peak assignment: ■, α-titanium; ○, anatase; ●, rutile; △, hydrogen titanate; *, distorted titanium.

morphologies previously observed. We attribute these changes in morphology to a progressive sintering reaction caused by the high calcination temperature. SEM images (Fig. 7) also show that the fibrous morphology and the porous structure consisting of fibrous particles are maintained until calcination at 600 °C. An enlarged cross-section image of the thin film calcined at 450 °C is shown in Fig. 7c. Although a dense phase is observed at the bottom of the thin film (i.e., at the interface between the nanotube phase and the titanium metal), the porous structure composed of fibrous particles is observed in the film itself. The cross-section image shown in Fig. 7c is similar to that of the as-grown sodium titanate nanotube thin film. Calcination at 750 °C changes the thin film into a porous thin film consisting of particles (with 50-nm average diameter) and interstitial pores (with 79-nm average size). Calcination at 900 °C yields larger particles and no pores.

XRD patterns (Fig. 8) show that calcination at 300 °C leads to the disappearance of the diffraction peaks observed before calcination attributed to titanate, and peaks attributed to anatase appear at 2θ=25.3° and 48.1° along with peaks attributed to α-titanium. As the calcination temperature increases to 450 and 600 °C, other peaks attributed to anatase appear at 2θ=37.7°, 53.7°, and 55.0°. The increase in the number of peaks attributed to anatase confirms the improved crystallinity after calcination.

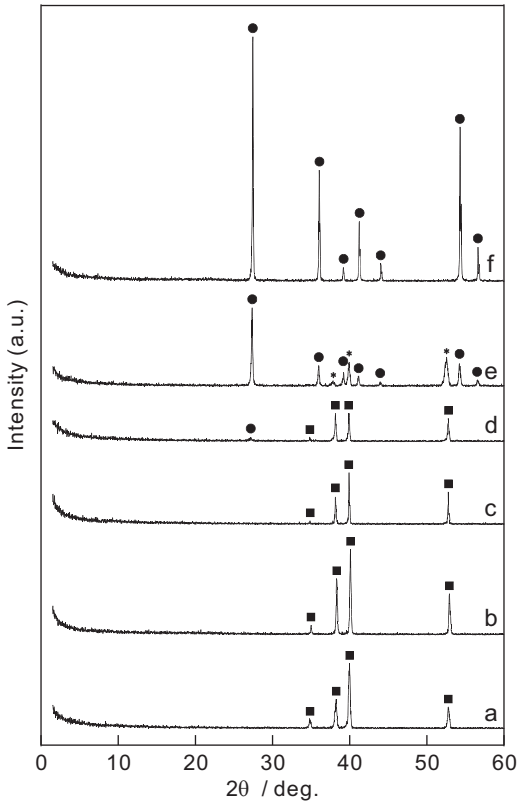

Fig. 9. XRD patterns of the raw titanium metal plate (a) and the calcined titanium metal plates at 300 °C (b), 450 °C (c), 600 °C (d), 750 °C (e), and 900 °C (f). Peak assignment: ■, α-titanium; ●, rutile; *, distorted titanium.

Calcination at 750 °C causes the peaks attributed to anatase to decrease and the peaks attributed to rutile (JCPDS no. 65-0191) to appear. Calcination at 900 °C causes only peaks attributed to rutile to appear. For comparison purposes, we calcined a titanium metal plate at 300–900 °C, and acquired XRD patterns to investigate the phase generated on the plate (Fig. 9). Calcination at 300 and 450 °C results only in peaks attributed to α-titanium to appear. It has already been reported that when a titanium metal plate is calcined, only the surface of the plate oxidizes and a rutile phase is generated [30]. Thus, in our study, we consider that the oxidized phase is so thin that we detect primarily the titanium metal below this phase. Calcination at 600 and 750 °C causes the peaks attributable to rutile to increase, which may be due to the increased thickness of the rutile phase that accompanies progress of the oxidation reaction from the surface of the plate into its inner regions. Together with the peaks attributed to the rutile, the other peaks appear on the low angle sides of the peaks of α-titanium, which we attribute as per Wang et al. [30] to a distorted titanium phase generated by the solution of oxygen into α-titanium and the resulting α-titanium lattice expansion. This distorted titanium phase also appears upon calcination of hydrogen titanate nanotube thin films at 600 and 750 °C (Figs. 8d and e). Calcination of a titanium metal plate at 900 °C causes peaks attributed to rutile to appear due to the advanced oxidation reaction.

Based on these results, we consider the following. Comparing the results shown in Figs. 8 and 9, the XRD peaks attributed to anatase that appear upon calcination of the hydrogen titanate nanotube thin film at 300–750 °C are attributed to the phase generated by the phase transition of hydrogen titanate. At 300 and 450 °C, an anatase nanotube thin film forms, whereas at 600 °C, an anatase nanowire thin film forms. At 750 °C, a porous thin film forms because of the connection of anatase particles.

At 900 °C, the thin film changes to a dense rutile thin film because of the densification and phase transition caused by the sintering of anatase nanoparticles.

In the above mentioned transformations from hydrogen titanate nanotube thin film into titanium dioxide nanotube or nanowire thin film, the crystal structure and morphology of the nanotubes that constitute the thin film change. The tendency of these changes is similar to that exhibited in the transformation reported by Morgado et al. [31] of hydrogen titanate nanotube particles into titanium dioxide nanotube and nanowire particles by calcination at up to 550 °C. However, the latter study focuses only on particles, whereas our study focuses on thin films and suggests that not only can the functions of nanotubes, nanowires, and nanoparticles themselves be used, but they may also be used as building blocks. Consequently, the nanospaces between titanium dioxide can be used as nanopores. In the abovementioned report of Kim et al. [21], titanium dioxide nanotube thin films are fabricated using the following method: (1) Titanate nanotube particles are synthesized; (2) a liquid in which the synthesized nanotube particles are dispersed is prepared; (3) nanotube particles are coated to a substrate by electrophoretic deposition (EPD) using the prepared liquid; and (4) the substrate is calcined to fix the nanotube particles onto it and transform titanate nanotubes into titanium dioxide nanotubes. However, this method involves complicated processes and results in poor adhesion of the thin film to the substrate. In contrast, our proposed method is very simple, in that it does not require the preparation of a nanotube dispersion liquid or EPD treatment of a substrate, as the nanotubes directly grow from the substrate. Furthermore, because of the direct growth of the nanotubes from the substrate, the fixing strength to the substrate is expected to be higher. Another advantage of the proposed method is that the thickness of the thin films produced (5 μm) is greater than that of the thin films reported by Miyauchi et al. [17] (several hundred nanometers) and Kim et al. [21] (2 μm). Furthermore, using the proposed method, we can fabricate thicker titanium dioxide nanotube thin films, as we have already obtained sodium titanate nanotube thin films as thick as 20 μm by hydrothermal reaction in 10 mol/L NaOH solution at 160 °C for 20 h [24].

We have also been examining the formation of nanotube thin films on the surfaces of implants. The coating of films to implants with complex shapes requires nanotube thin films with uniform and controlled thickness, and a high fixing strength [32] to the implants. Therefore, the method proposed in the present study has excellent potential for these biomedical applications.

Acknowledgments

This research was partially supported by KAKENHI (16685021, 19750172).

Appendix A. Supplementary material

Supplementary data associated with this article can be found in the online version at doi:10.1016/j.jssc.2009.10.028.

References

[1] H. Imai, Y. Takei, K. Shimizu, M. Matsuda, H. Hirashima, J. Mater. Chem. 9 (1999) 2971–2972.
[2] S. Yamanaka, T. Hamaguchi, H. Muta, K. Kurosaki, M. Uno, J. Alloys Compds. 373 (2004) 312–315.
[3] J.H. Jung, H. Kobayashi, K.J.C. van Bommel, S. Shinkai, T. Shimizu, Chem. Mater. 14 (2002) 1445–1447.
[4] H. Shin, D.-K. Jeong, K. Lee, M.M. Sung, J. Kim, Adv. Mater. 16 (2004) 1197–1200.
[5] J.M. Macak, H. Tsuchiya, P. Schmuki, Angew. Chem. Int. Ed. 44 (2005) 2100–2102.
[6] S. Sharma, O.K. Varghese, G.K. Mor, T.J. LaTempa, N.K. Allam, C.A. Grimes, J. Mater. Chem. 19 (2009) 3895–3898.
[7] T. Kasuga, M. Hiramatsu, A. Hoson, T. Sekino, K. Niihara, Langmuir 14 (1998) 3160–3163.
[8] T. Kasuga, M. Hiramatsu, A. Hoson, T. Sekino, K. Niihara, Adv. Mater. 11 (1999) 1307–1311.
[9] Q. Chen, W. Zhou, G. Du, L.-M. Peng, Adv. Mater. 14 (2002) 1208–1211.
[10] H. Tokudome, M. Miyauchi, Chem. Lett. 33 (2004) 1108–1109.
[11] Z. Jiang, F. Yang, N. Luo, B.T.T. Chu, D. Sun, H. Shi, T. Xiao, P.P. Edwards, Chem. Commun. (2008) 6372–6374.
[12] S. Uchida, R. Chiba, M. Tomiha, N. Masaki, M. Shirai, Electrochemistry 70 (2002) 418–420.
[13] D.V. Bavykin, A.A. Lapkin, P.K. Plucinski, J.M. Friedrich, F.C. Walsh, J. Phys. Chem. B 109 (2005) 19422–19427.
[14] H. Tokudome, M. Miyauchi, Angew. Chem. Int. Ed. 44 (2005) 1974–1977.
[15] S. Kubota, K. Johkura, K. Asanuma, Y. Okouchi, N. Ogiwara, K. Sasaki, T. Kasuga, J. Mat. Sci. Mater. Med. 15 (2004) 1031–1035.
[16] A. Thorne, A. Kruth, D. Tunstall, J.T.S. Irvine, W. Zhou, J. Phys. Chem. B 109 (2005) 5439–5444.
[17] M. Miyauchi, H. Tokudome, Y. Toda, T. Kamiya, H. Hosono, Appl. Phys. Lett. 89 (2006) 043114.
[18] H. Tokudome, M. Miyauchi, Chem. Commun. (2004) 958–959.
[19] T. Kasuga, Jpn. Kokai Tokkyo Koho (2003) P2003-220127A.
[20] R. Ma, T. Sasaki, Y. Bando, J. Am. Chem. Soc. 126 (2004) 10382–10388.
[21] G.-S. Kim, S.G. Ansari, H.-K. Seo, Y.-S. Kim, H.-S. Shin, J. Appl. Phys. 101 (2007) 024314.
[22] Z.R. Tian, J.A. Voigt, J. Liu, B. Mckenzie, H. Xu, J. Am. Chem. Soc. 125 (2003) 12384–12385.
[23] B. Chi, E.S. Victorio, T. Jin, J. Nanosci. Nanotechnol. 7 (2007) 668–672.
[24] M. Yada, Y. Inoue, M. Uota, T. Torikai, T. Watari, I. Noda, T. Hotokebuchi, Langmuir 23 (2007) 2815–2823.
[25] Y. Guo, N.-H. Lee, H.-G. Oh, C.-R. Yoon, K.-S. Park, H.-G. Lee, K.-S. Lee, S.-J. Kim, Nanotechnology 18 (2007) 295608.
[26] Y. Inoue, M. Uota, T. Torikai, T. Watari, I. Noda, T. Hotokebuchi, M. Yada, J. Biomed. Mater. Res. A, in press doi:10.1002/jbm.a.32456.
[27] A. Nakahira, W. Kato, M. Tamai, T. Isshiki, K. Nishio, H. Aritani, J. Mater. Sci. 39 (2004) 4239–4245.
[28] C.-C. Tsai, H. Teng, Chem. Mater. 18 (2006) 367–373.
[29] H.Y. Zhu, Y. Lan, X.P. Gao, S.P. Ringer, Z.F. Zheng, D.Y. Song, J.C. Zhao, J. Am. Chem. Soc. 127 (2005) 6730–6736.
[30] X.-X. Wang, W. Yan, S. Hayakawa, K. Tsuru, A. Osaka, Biomaterials 24 (2003) 4631–4637.
[31] E. Morgado Jr., M.A.S. de Abreu, O.R.C. Pravia, B.A. Marinkovic, P.M. Jardim, F.C. Rizzo, A.S. Araújo, Solid State Sci. 8 (2006) 888–900.
[32] H.M. Kim, F. Miyaji, T. Kokubo, J. Mater. Sci. Mater. Med. 8 (1997) 341–347.